CERTAIN ASPECTS OF THE CALIBRATION AND RESOLUTION OF SLOW NEUTRON SPECTROMETERS

L. Q. AMARAL, L. A. VINHAS, C. RODRIGUEZ AND S. B. HERDADE

PUBLICAÇÃO IEA N.º 175
Setembro — 1968

INSTITUTO DE ENERGIA ATÔMICA
Caixa Postal 11049 (Pinheiros)
CIDADE UNIVERSITÁRIA "ARMANDO DE SALLES OLIVEIRA"
SÃO PAULO — BRASIL

CERTAIN ASPECTS OF THE CALIBRATION AND RESOLUTION OF SLOW NEUTRON SPECTROMETERS

L.Q. Amaral, L.A. Vinhas, C. Rodriguez and S.B. Herdade

Divisão de Física Nuclear
Instituto de Energia Atômica
São Paulo - Brasil

Publicação IEA Nº 175
Setembro - 1968

---

* Publicado em Nuclear Instruments and Methods 63 (1968) 13-22; (C) North-Holland Publishing Co., Amsterdam.

Comissão Nacional de Energia Nuclear

Presidente: Prof. Uriel da Costa Ribeiro

Universidade de São Paulo

Reitor: Prof.Dr. Luis Antonio da Gama e Silva

Instituto de Energia Atômica

Diretor: Prof. Rômulo Ribeiro Pieroni

Conselho Técnico-Científico do IEA

Prof.Dr. José Moura Gonçalves } pela USP
Prof.Dr. José Augusto Martins }
Prof.Dr. Rui Ribeiro Franco } pela CNEN
Prof.Dr. Theodoreto H.I. de Arruda Souto }

Divisões Didático-Científicas

Divisão de Física Nuclear -
Chefe: Prof.Dr. Marcello D.S. Santos

Divisão de Radioquímica -
Chefe: Prof.Dr. Fausto Walter de Lima

Divisão de Radiobiologia -
Chefe: Prof.Dr. Rômulo Ribeiro Pieroni

Divisão de Metalurgia Nuclear -
Chefe: Prof.Dr. Tharcísio D.S. Santos

Divisão de Engenharia Química -
Chefe: Lic. Alcídio Abrão

Divisão de Engenharia Nuclear -
Chefe: Engº Pedro Bento de Camargo

Divisão de Operação e Manutenção de Reatores -
Chefe: Engº Azor Camargo Penteado Filho

Divisão de Física de Reatores -
Chefe: Prof.Dr. Paulo Saraiva de Toledo

Divisão de Ensino e Formação -
Chefe: Prof. Rui Ribeiro Franco

NUCLEAR INSTRUMENTS AND METHODS 63 (1968) 13–22; © NORTH-HOLLAND PUBLISHING CO.

CERTAIN ASPECTS OF THE CALIBRATION AND RESOLUTION OF SLOW NEUTRON SPECTROMETERS

L. Q. AMARAL, L. A. VINHAS, C. RODRIGUEZ and S. B. HERDADE

Nuclear Physics Division, Instituto de Energia Atômica, Cidade Universitaria, São Paulo, Brasil

Received 8 January 1968 and in revised form 27 February 1968

The method of calibrating and determining the resolution of slow neutron spectrometers by the measurement of Bragg breaks is discussed. The folding of a Gaussian resolution function with a linear function presenting a sharp break is analytically studied. The ratio between the resulting "break width" and the resolution width is determined; in practical cases it is 1.0645. A relation between the mean abscissa, corresponding to the half-height of the resulting curve, and the true position of the break is given; they coincide only for symmetrical breaks. The effect of a Gaussian resolution in the transmission, inverse transmission, and total cross section, is theoretically evaluated for the iron (110) Bragg cut-off, for many resolution widths and several sample thicknesses. It is concluded that the analysis of the measured transmission curve gives the most direct and accurate result.

The characteristics of a curved-slit slow neutron chopper and time-of-flight spectrometer built at the IEA are presented. The time resolution for the present conditions of geometry, with a very small detecting area, is 1% for a 3 m flight path and 4.046 Å neutrons. A calibration independent of the chopper speed, desirable when a wide energy range must be covered, has been attained within the precision of 4 μsec. The spectrometer can be used from 0.5 Å up to 12 Å for total cross section measurements.

1. Introduction

A curved-slit slow neutron chopper, built following a design developed[1]) at the Swedish Atomenergi, is presently being used in a time-of-flight spectrometer operating at the IEA swimming pool 5 MW research reactor, for measuring total neutron cross sections.

This paper, besides presenting some characteristics of the spectrometer, discusses the method of calibrating and determining the resolution of slow neutron spectrometers by the measurement of Bragg breaks that appear in the total cross section of polycrystalline substances. The spectrometer resolution affects the theoretically sharp break, so that, in the observed curve, the edges become rounded and the vertical discontinuity assumes a finite slope; the problem of determining the exact calibration point and the relation between the resolution width and the observed slope has not yet been systematically treated, although the method has often been used in several alternative ways.

A measurement of the total cross section curve of a polycrystalline sample, by transmission, is recommended by Hughes[2]). The method has been considered in more detail by Egelstaff[3]), who made the study of the reciprocal transmission on a logarithmic scale, and recommends the computation of the mean wavelength corresponding to the half-height of the observed break for each resolution value. A very accurate study of calibration of a time-of-flight spectrometer was made by Deruytter et al., who used[4]) Egelstaff's method and also a method of equivalent areas[5]) for defining the calibration point in the measured transmission curve. The reciprocal transmission in a linear scale and the transmitted intensity have also been used[6]) for calibrating. When a thick Be refrigerated filter is used for obtaining a cold neutron beam, the transmitted spectrum can be approximated by a triangular step function; in this case the calibration and resolution can be obtained by its direct measurement, as studied by Larsson et al.[7]).

The problem has been retaken in the present work aiming at a more general solution and a complete understanding of the possibilities of the method. This question has been treated from two points of view: the formal problem of folding a Gaussian resolution function with a linear function presenting a sharp break and the theoretical evaluation of the resolution effect in the particular case of the iron (110) Bragg cut-off.

In our spectrometer special care was taken to obtain a calibration independent of the chopper speed, because in total cross section measurements it is often desirable to change the chopper speed for covering different neutron energy ranges. For these measurements, a small beam area had to be defined, because of the size of some available samples, for instance rare earth oxides[8]). The theoretical resolution for this experimental arrangement has been calculated in detail, since for our present geometry the problem had not been fully treated before.

2. Detailed analysis of the "Bragg break" method

2.1. Gaussian function applied to a linear function presenting a break

Let us consider the general problem of a Gaussian resolution function applied to a linear function $f(x)$ that has a discontinuity at the point $x = b$, as shown in fig. 1. This linear function is given by

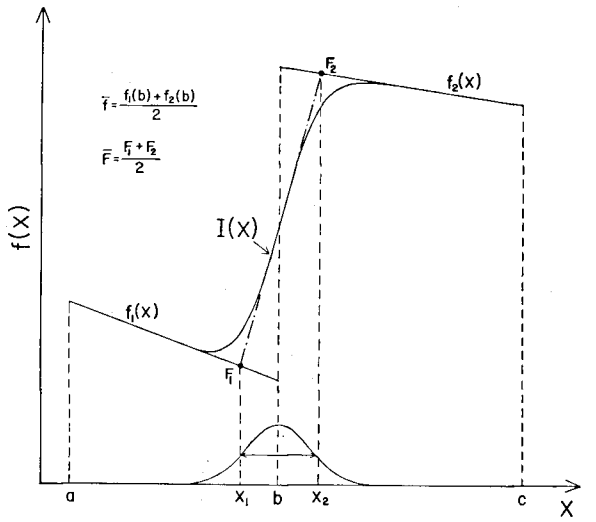

Fig. 1. A Gaussian function is applied to the linear function $f(x)$, that has a sharp break at $x=b$; the resulting break is described by $I(x)$. The abcissa corresponding to the mean value $\bar{F}$ and the break width $\delta x=x_2-x_1$ can be graphically determined.

$$f(x)=\begin{cases} f_1(x)=A_1x+B_1, & \text{for } 0\leqq a\leqq x\leqq b,\\ f_2(x)=A_2x+B_2, & \text{for } b\leqq x\leqq c,\\ 0, & \text{for } x<a \text{ or } x>c.\end{cases}$$

The variable x can be, in the case of slow neutron spectrometers, the neutron wavelength, velocity, or time-of-flight. The point b is a Bragg cut-off; the points a and c define the interval where $f(x)$ can be considered a linear function of x, but do not represent necessarily physical discontinuities.

The normalized resolution function is given by

$$R(x-x_0)=(\pi^{\frac{1}{2}}\Delta x)^{-1}\exp[-\{(x-x_0)/\Delta x\}^2],$$

and its width at half height is $\Gamma=2(\ln 2)^{\frac{1}{2}}\Delta x$.

We are interested in the function

$$I(x)=\int_{-\infty}^{+\infty} f(x_0)R(x-x_0)\,dx_0,$$

given by

$$I(x)=\int_a^x f_1(x_0)R(x-x_0)\,dx_0+$$
$$+\int_x^b [f_1(x_0)-f_2(x_0)]R(x-x_0)\,dx_0+$$
$$+\int_x^c f_2(x_0)R(x-x_0)\,dx_0.$$

Integrating and defining the variables

$$y_1=(x-a)/\Delta x,\quad y_2=(c-x)/\Delta x \quad\text{and}\quad z=(x-b)/\Delta x,$$

it results

$$I(x)=\tfrac{1}{2}\Delta x\cdot\pi^{-\frac{1}{2}}[(A_2-A_1)\exp(-z^2)+$$
$$+A_1\exp(-y_1^2)-A_2\exp(-y_2^2)]+$$
$$+\tfrac{1}{2}\{f_1(x)\operatorname{erf}(y_1)+f_2(x)\operatorname{erf}(y_2)\}+$$
$$+\tfrac{1}{2}\{f_2(x)-f_1(x)\}\operatorname{erf}(z), \qquad (1)$$

where $\operatorname{erf}(\eta)$ is the error function defined by

$$\operatorname{erf}(\eta)=2\cdot\pi^{-\frac{1}{2}}\int_0^{\eta}\exp(-t^2)\,dt.$$

When $f(x)$ represents the cold neutron spectrum transmitted through a thick Be filter the simplifications

$$A_1=B_1=0,\quad A_2=1/(c-b)\quad\text{and}\quad B_2=c/(c-b),$$

lead to the discussion made by Larsson et al.[7]), having the neutron time-of-flight as variable x.

When $f(x)$ represents the transmission of a polycrystalline sample with intervals $(c-b)$ and $(b-a)$ sufficiently large compared to Δx, the behaviour of $f(x)$ for $x<a$ or $x>c$ does not influence the shape of the observed break, described in this case by the simplified expression

$$I(x)=\tfrac{1}{2}\{f_1(x)+f_2(x)\}+\tfrac{1}{2}\pi^{-\frac{1}{2}}(A_2-A_1)\Delta x\cdot\exp(-z^2)+$$
$$+\tfrac{1}{2}\{f_2(x)-f_1(x)\}\operatorname{erf}(z),$$

that reduces to $f_1(x)$ for $x\ll b-\Delta x$ and to $f_2(x)$ for $x\gg b+\Delta x$.

Let us call $\bar{f}$ the mean value of the function $f(x)$ at the break position and H the break height, which can be positive or negative, defined by the relations

$$\bar{f}=\tfrac{1}{2}\{f_1(b)+f_2(b)\}\quad\text{and}\quad H=f_1(b)-f_2(b).$$

Changing to the new variable z, that expresses the distance between an abcissa x and the break position b, in units of Δx, the resulting break is given by

$$I(z)=\bar{f}+\tfrac{1}{2}(A_1+A_2)\Delta x\cdot z+$$
$$+\tfrac{1}{2}\pi^{-\frac{1}{2}}(A_2-A_1)\Delta x\cdot\exp(-z^2)-\tfrac{1}{2}H\operatorname{erf}(z)+$$
$$+\tfrac{1}{2}(A_2-A_1)\Delta x\cdot z\operatorname{erf}(z). \qquad (2)$$

For finite resolution values, $\Delta x\neq 0$, the value observed at the break position,

$$I(b)=\bar{f}+\tfrac{1}{2}\pi^{-\frac{1}{2}}(A_2-A_1)\Delta x, \qquad (3)$$

is equal to $\bar{f}$ only for a symmetrical break, when $A_1=-A_2$. Depending on the relative inclinations of the straight lines, the abcissa x', corresponding to the mean value $\bar{f}$, will be shifted towards values smaller or bigger than b, and can be found through the related z' by solving the transcendental equation $I(z')=\bar{f}$.

The importance of this shift is given by

$$\tfrac{1}{2}\pi^{-\frac{1}{2}}(A_2-A_1)\Delta x/\bar{f}.$$

Deruytter et al.[5]) have measured the transmission of an iron sample and have taken as true break position a flight time such that on both sides the areas corresponding to the difference between $f(x)$ and $I(x)$ are equal. This method is always valid if the following areas are equal:

$$S_1=\int_a^b[f_1(x)-I(x)]\,dx \quad \text{and} \quad S_2=\int_b^c[I(x)-f_2(x)]\,dx.$$

Conserving the hypothesis that the intervals are much larger than Δx, it results by integration

$$S_1=\tfrac{1}{2}\pi^{-\frac{1}{2}}H\Delta x+\tfrac{1}{8}(A_1-A_2)(\Delta x)^2 \quad \text{and}$$
$$S_2=\tfrac{1}{2}\pi^{-\frac{1}{2}}H\Delta x-\tfrac{1}{8}(A_1-A_2)(\Delta x)^2.$$

It can be seen that only in the case of a symmetrical break the method of equivalent areas leads to the exact calibration point, and the percentual error of this method is given by

$$\tfrac{1}{2}\pi^{\frac{1}{2}}(A_2-A_1)\Delta x/H.$$

In fig. 1 a typical observed break is shown, for the case in which A_1 and A_2 are both negative. Let us determine analytically the quantities that can be graphically obtained.

Making the second derivative of $I(x)$ equal to zero, the inflexion point of the resulting curve is

$$z_i=\tfrac{1}{2}(A_1-A_2)\Delta x/H \text{ or } x_i=b+\tfrac{1}{2}(A_1-A_2)(\Delta x)^2/H. \quad (4)$$

The value z_i, that expresses the shift of the inflexion point to the break position, gives thus the order of magnitude of the distortion in the resulting break due to the asymmetry of $f(x)$.

It is then possible to obtain the equation of the straight line tangent to the observed break at the inflexion point and to determine the intersections x_1 and x_2 (through the related z_1 and z_2) with the function $f(x)$ and the corresponding values F_1 and F_2.

Analytical calculations lead to:

$$z_1=\frac{-\{1+\operatorname{erf}(z_i)\}}{2\pi^{-\frac{1}{2}}\exp(-z_i^2)+2z_i[1+\operatorname{erf}(z_i)]}, \quad (5)$$

$$z_2=\frac{+\{1-\operatorname{erf}(z_i)\}}{2\pi^{-\frac{1}{2}}\exp(-z_i^2)-2z_i[1-\operatorname{erf}(z_i)]}. \quad (6)$$

From these two expressions it is seen that z_1 and z_2 are anti-symmetrical functions of z_i in relation to each other, or

$$z_1(-z_i)=-z_2(z_i).$$

The resulting "break width" δx is defined by

$$\delta x=x_2-x_1=(z_2-z_1)\Delta x,$$

or, in terms of the half-width of the Gaussian resolution function,

$$\delta x/\Gamma=(z_2-z_1)/\{2(\ln 2)^{\frac{1}{2}}\}. \quad (7)$$

From the symmetrical properties of z_1 and z_2, it follows that this ratio is an even function of z_i.

It is also possible to determine the abcissa $\bar{x}$ (through the related $\bar{z}$) that corresponds to the mean observed value

$$\bar{F}=\tfrac{1}{2}(F_1+F_2),$$

by solving the transcendental equation $I(\bar{z})=\bar{F}$, that reduces to

$$K(2\bar{z}-z_1-z_2)-z_i[2\pi^{-\frac{1}{2}}\exp(-\bar{z}^2)+$$
$$+2\bar{z}\operatorname{erf}(\bar{z})+z_1-z_2]-\operatorname{erf}(\bar{z})=0,$$

where $K=\tfrac{1}{2}(A_1+A_2)\Delta x/H$ is a positive parameter, always $\geqq|z_i|$.

For a symmetrical break,

$$z_i=\bar{z}=z'=0 \text{ or } x_i=\bar{x}=x'=b \text{ and } I(x_i)=\bar{F}=\bar{f}=I(b).$$

In this case it comes out also that

$$z_1=-\tfrac{1}{2}\pi^{\frac{1}{2}}, \qquad z_2=+\tfrac{1}{2}\pi^{\frac{1}{2}}$$

and thus

$$\delta x/\Gamma=\pi^{\frac{1}{2}}/\{2(\ln 2)^{\frac{1}{2}}\}\cong 1.0645, \quad (8)$$

result already given by Larsson et al.[7]) for the particular case $A_1=A_2=0$.

For $\Delta x\to 0$ it results also $z_i\to 0$, but in this case x_1 and $x_2\to b$ and $\delta x\to 0$.

In the general case, when $A_1\neq A_2$, only the inflexion point is easily calculated from eq. (4). For all other quantities calculations have been performed in a digital IBM-1620-II computer, expanding $\operatorname{erf}(\eta)$ in series, with the inflexion point z_i as variable.

In fig. 2 the ratio $\delta x/\Gamma$ is presented as a function of z_i.

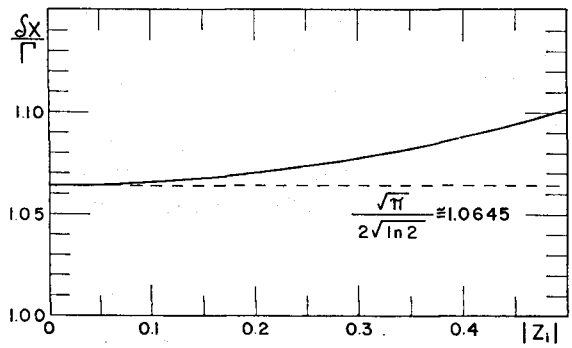

Fig. 2. The ratio between the break width and the full width at half maximum of the Gaussian resolution, as a function of the inflexion point z_i. Neglecting second power contribution of z_i, this ratio is constant.

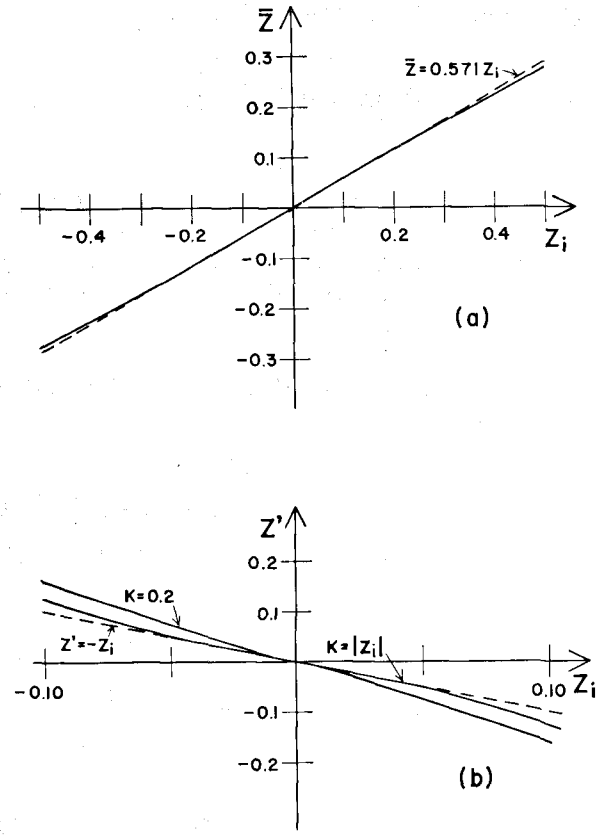

Fig. 3. a. Curve of $\bar{z}$ as a function of the inflexion point z_i, obtained by solving the transcendental equation $I(\bar{z},z_i,K)=\bar{F}$. Results show that $\bar{z}$ is almost insensible to the parameter K;
b. Curve of z' as a function of the inflexion point z_i, obtained by solving the transcendental equation $I(z',z_i,K)=\bar{f}$. Results are shown for $K=|z_i|$ and for $K=0.2$.
The dotted lines are the results obtained when second power contributions of z_i are neglected.

In fig. 3a, b, curves of $\bar{z}$ and z' as functions of z_i, having K as parameter, are shown. The transcendental equations have been solved by the Newton-Raphson method. z' has opposite sign to z_i and shows a significant variation with K, while $\bar{z}$ has the same sign as z_i and is almost insensible to K; both are odd functions of z_i.

The interesting and simple results observed in these curves for small values of $|z_i|$ can be analytically obtained by neglecting second power contributions of z_i. This approximation leads to

$$z_1+z_2\cong z_i(\pi-2) \quad \text{and} \quad z_2-z_1\cong \pi^{\frac{1}{2}},$$

showing that for $|z_i|\leqq 0.1$, the ratio $\delta x/\Gamma$ is constant and eq. (8) is valid.

When K and z_i are of the same order this approximation leads to the simplified relations

$$z'\cong -z_i \quad \text{and} \quad \bar{z}\cong(\tfrac{1}{2}\pi-1)z_i.$$

So, for conditions such that $|z_i|\leqq 0.2$, which is actually the case for Bragg breaks, the true calibration point b is related to the mean observed value $\bar{x}$ by

$$b=\bar{x}+(\tfrac{1}{2}\pi-1)\{\tfrac{1}{2}(A_2-A_1)/H\}[\Gamma/\{2(\ln 2)^{\frac{1}{2}}\}]^2. \quad (9)$$

The values A_1, A_2 and H are experimentally determined, at least in a first approximation, from a break measurement. Through the experimentally determined values of δx and $\bar{x}$, the resolution width Γ and the calibration point can then be obtained by using the simple eqs. (8) and (9).

If $|A_1|>|A_2|$, that is the case for the last Bragg cut-off, after which coherent scattering no longer exists, $b<\bar{x}$.

Calculations have been performed for arbitrary breaks, by using eq. (2) and the results graphically obtained from the plotted curves agree very well with the ones expected from eq. (9).

2.2. Theoretical evaluation of the resolution effect on the (110) Bragg break of iron

The results that would be experimentally obtained while measuring the iron (110) Bragg cut-off at 4.046 Å have been evaluated by a digital IBM-1620-II computer calculation. The theoretical total cross section $\sigma_t(\lambda)$ as a function of wavelength used in this evaluation was calculated[9]) taking into account all the partial cross sections (coherent elastic and inelastic, absorption, incoherent elastic and inelastic), and using a Debye temperature of 400°K.

The observed transmission of a sample containing n atoms/b, given by the ratio between the transmitted and the incident neutron beam, depends on the spectrometer resolution according to

$$T_{\text{obs}}(\lambda_0)=\frac{\int_{-\infty}^{+\infty}\exp[-n\sigma_t(\lambda)]R(\lambda-\lambda_0)\,\mathrm{d}\lambda}{\int_{-\infty}^{+\infty}R(\lambda-\lambda_0)\,\mathrm{d}\lambda}. \quad (10)$$

Calculations of T_{obs}, $(T_{\text{obs}})^{-1}$, $\ln(T_{\text{obs}})^{-1}$ and $\sigma_{\text{obs}}=n^{-1}\ln(T_{\text{obs}})^{-1}$ have been performed by numerical methods in the range 3.0 Å to 5.0 Å, for different resolution widths and also for various values of n, in order to determine the influence of the sample thickness in the observed break. The resolution function has been considered of Gaussian shape; actually the resolution width varies with λ, but this has not been taken into account, since in the interval of interest this variation is negligible.

Curves of T_{obs} and σ_{obs}, for two resolutions, are shown in fig. 4. The mean wavelength, corresponding to the half-height, and the width of the observed break were graphically determined for the four calculated functions, by the usual method of extrapolating the two branches of the curve and finding the intersections with the tangent at the inflexion point. Some of the results are shown in table 1.

It seems clear from the results obtained that the analysis of the observed transmission gives the most direct and accurate calibration, since this is the function where the mean wavelength is closest to the Bragg cut-off; in fig. 4 it can also be seen that the observed transmission is more suitable for the analysis than the cross section. The spectrometer resolution is actually applied on the theoretical transmission, and the others are inverse functions. Thus the results from section 2.1 apply only to the transmission; in relation to the theoretical cut-off, the mean wavelength is shifted towards longer values in the observed transmission, as predicted before, and in the opposite direction, towards shorter wavelengths, in the other functions.

There are some difficulties in making a straight line fit in the region where $\lambda < 4.046$ Å, due to the dependence of the coherent scattering with λ^2, and regarding this aspect the function $\ln(T^{-1})$ may present some advantages. However, the theoretical transmission function is the one closer to be symmetrical, and this favours its use.

Because of these reasons, the observed transmission presents also the advantage of having the smallest sensitivity to the n value of the particular sample used in the measurement.

TABLE 1

Mean wavelength $\bar{\lambda}$, corresponding to the half-height of the resulting break; results graphically obtained from the four calculated functions. The precision is about 0.03%. The Bragg cut-off is at 4.046 Å; the transmission is the most convenient function to analyse.

n (atoms/b)	Γ (Å)	Mean wavelength $\bar{\lambda}$ (Å) in T_{obs}	in $(T_{obs})^{-1}$	in $\ln(T_{obs})^{-1}$	in σ_{obs}
0.089	0.10	4.046	4.015	4.030	4.030
0.089	0.20	4.047	3.985	4.015	4.016
0.089	0.30	4.048	3.963	4.005	4.005
0.089	0.40	4.049	3.945	3.995	3.995
0.150	0.20	4.048	3.950	3.997	3.997

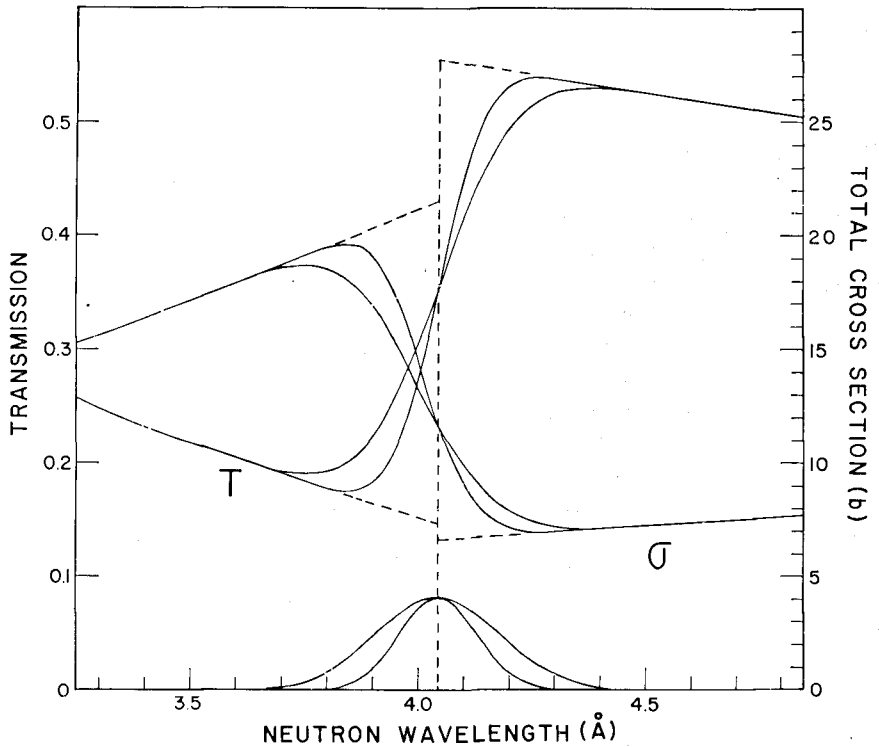

Fig. 4. Theoretical evaluation of the resolution effect on the iron (110) Bragg cut-off. Curves of T_{obs} and σ_{obs} are presented for two resolution widths, 0.20 and 0.32 Å, and for a sample containing 0.089 atoms/b. It is clearly seen that the transmission curve is more symmetrical about the true cut-off position.

Making a straight line fit to the theoretical transmission, the expected shifts from eq. (9) agree with the graphical results of table 1 within the precision of the graphical method, which is about 0.03%. The widths of the applied resolutions agree with the results obtained from eq. (8) within 1%, because there is in this case a larger uncertainty in the graphical method.

This agreement shows that by measuring the transmission of polycrystalline samples and using the simple derived eqs. (8) and (9), it is possible to calibrate and to determine experimentally the resolution of slow neutron spectrometers in a very accurate way; using this method it is not necessary to perform all the computations for each particular resolution width.

The sample thickness should be chosen to give the best transmission measurement; the conditions of maximum observed break in the transmission is achieved by

$$n^* = \{\ln(\sigma_{max}/\sigma_{min})\}/(\sigma_{max}-\sigma_{min}), \qquad (11)$$

where σ_{max} and σ_{min} are, respectively, the maximum and minimum cross section values of a Bragg break. For the iron (110) cut-off, $n^* \cong 0.08$ atoms/b.

In an actual transmission measurement, there is a factor that must be multiplied by the resolution function in the numerator and denominator of eq. (10), which contains the effects depending on λ that modify the neutron spectrum. This may cause a small additional distortion towards longer wavelengths.

3. Results for a chopper and time-of-flight facility

3.1. The spectrometer

The principle of operation of the slow neutron chopper and time-of-flight spectrometer is well known[10]; the chopper parameters have been chosen[1]) for a convenient utilization in inelastic scattering experiments using the Be filter technique. The chopper[11]) consists essentially of a cylindrical rotor of radius $r = 5$ cm and length 14 cm, which contains nine cadmium covered steel plates 0.5 mm thick separated by aluminium spacers forming 10 curved slits of width $2d = 0.3968$ cm and nominal radius of curvature $R_0 = 74.5$ cm. The chopper total opening is 11 cm × 4.5 cm. The remaining volume of the cylinder is filled with B_4C mixed with araldite in approximately equal amounts. A universal electric motor connected by elastic coupling to the rotor axis can rotate the chopper with speeds up to 15000 rpm.

An electromagnetic pick-up provides a signal for each chopper revolution; however, the wave form of this signal does not satisfy the requirements of the TMC time analyser trigger input, besides presenting an undesirable variation with the chopper speed. A pulse shape circuit[11]), triggered by the pick-up signal at a level of 15 mV, gives the pulse that is utilized both to start the multichannel analyser and to control the chopper speed within 0.5%. Careful measurements of the exact trigger point showed a variation of less than 2 μsec in the zero time over the total range of chopper speeds. This error is small and can be neglected when considering the calibration problem.

The pick-up position can be manually adjusted, so that the rotating magnet passes right in front of the fixed pick-up coil in the exact moment a neutron burst is formed in the center of the chopper, defining the zero time for the neutrons. If there is an angular shift $\Delta\phi$ between the pick-up coil and the magnet at this exact moment, the triggering pulse is sent a fraction of revolution later (or earlier), corresponding to a time difference $\Delta t_1 = \Delta\phi/\omega$, where ω is the chopper angular velocity. The pick-up position must be carefully adjusted, in order to make $\Delta\phi = 0$, thus ensuring a correct zero time.

In the direct beam experimental arrangement[11]), a collimator defines a 2.5×1.0 cm^2 beam area at the chopper entrance, much smaller than the total chopper opening. The position of the neutron detector, a 1″ thick BF_3, defines the flight path and can be easily changed; flight paths of 1.5 and 3.0 m are mostly used.

3.2. Theoretical resolution

Different contributions must be considered in the study of the overall resolution of the chopper and time-of-flight spectrometer: one that depends on the parameters and speed of the chopper and on the geometry of the system, δt_ω, and another due to the channel width δt_a of the time analyser and to the detector finite thickness. If all contributions are added as Gaussian functions, the total spectrometer resolution is

$$\delta t = \{(\delta t_\omega)^2 + (l/v)^2 + (\delta t_a)^2\}^{\frac{1}{2}}, \qquad (12)$$

where l is the detector effective thickness for neutrons of velocity v.

The contribution δt_ω will be calculated for our geometry. The chopper has a transmission $T(\alpha,v)$, function of the neutron velocity and of the angle of incidence α between the neutron path and the chopper slits; this function has been analytically determined[1,12]) for small α values. For the study of the resolution we can restrict ourselves to neutrons of velocity $v_0 = 2\omega R_0$ of maximum transmission; $T(\alpha,v_0)$ is a triangle of basis $2d/r$.

As the chopper rotates, its slits sweep the neutron emitting area, defining an angle α' that varies with time. The angular width of the chopper burst is determined by

the chopper opening and by the geometrical collimation $2D/L$, where $2D$ is the emitting (or detecting) surface and L its distance to the chopper center.

Assuming a constant neutron flux over the entire effective emitting surface and a constant efficiency over the effective detector surface, expressed by

$$I_0(\alpha) = \begin{cases} 1 & \text{for } \alpha \leqq |D/L|, \\ 0 & \text{for } \alpha \geqq |D/L|, \end{cases}$$

the transmitted intensity $I(\alpha', v_0)$ will be given by integrating the product of $I_0(\alpha)$ by $T(\alpha-\alpha')$, as is shown in fig. 5a. The resultant resolution function depends on the relative widths of the triangle and of the rectangle.

We shall make the analysis for the case in which $2D/L \leqq d/r$, that has not been treated before, since it represents a large loss in intensity with a comparatively small gain in resolution; this is the case for our present geometry, where, however, the intensity is not a serious problem, since direct beam experiments are being performed.

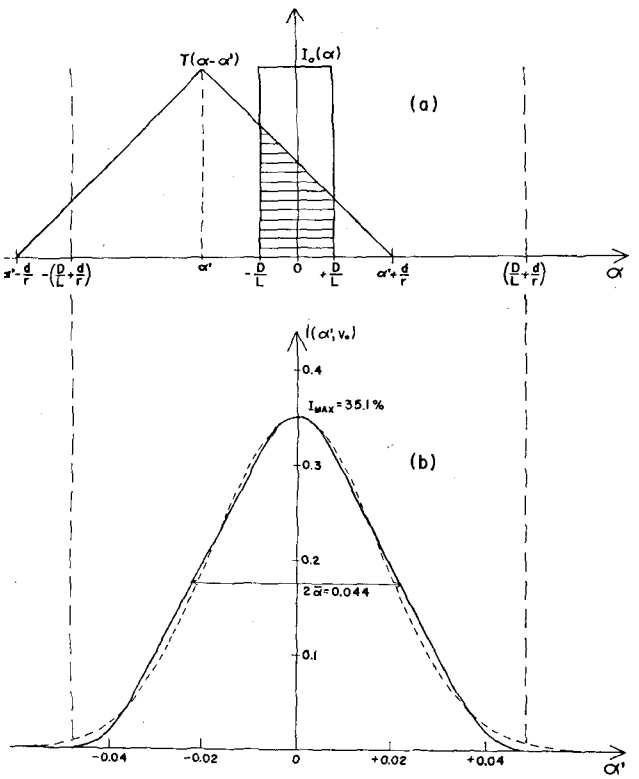

Fig. 5. a. Rectangular function $I_0(\alpha)$ representing the detecting area swept by the triangular function $T(\alpha-\alpha')$. The dashed area represents the function $I(\alpha', v_0)$;
b. Resolution function $I(\alpha', v_0)$ for a 1.5 m flight path. The dotted line shows the approximation by a Gaussian function of same area.

Normalizing the area of $T(\alpha-\alpha')$ to unity, the integration gives in this case

$$\begin{cases} I(\alpha') = 1-(r/d)^2[\{(d/r)-(D/L)\}^2+\alpha'^2], \\ \qquad \text{for } 0 \leqq |\alpha'| \leqq D/L; \\ I(\alpha') = (r/d)^2 2(D/L)\{(d/r)-\alpha'\}, \\ \qquad \text{for } D/L \leqq |\alpha'| \leqq (d/r)-(D/L); \\ I(\alpha') = \tfrac{1}{2}(r/d)^2\{(d/r)-\alpha'+(D/L)\}^2, \\ \qquad \text{for } (d/r)-(D/L) \leqq |\alpha'| \leqq (d/r)+(D/L). \end{cases}$$

The maximum transmission, $I_{\max} = I(\alpha'=0)$, can reach only 75%.

An analytical determination of the full width at half maximum $2\bar{\alpha}$ of this resolution function shows that two cases must be considered, because $I(\bar{\alpha})$ can fall in different branches of the curve. Results are as follows:

(a). $2\bar{\alpha} = 2\{(d/r)+(D/L)\}-2[(D/L)\{(2d/r)-(D/L)\}]^{\frac{1}{2}}$, for $\frac{4}{5}d/r \leqq 2D/L \leqq d/r$

and hence it is in the interval $1.2\, d/r \leqq 2\bar{\alpha} \leqq (3-\sqrt{3})d/r$;

(b). $2\bar{\alpha} = (d/r)+(\frac{1}{2}D/L)$, for $2D/L \leqq \frac{4}{5}d/r$

and hence it is in the interval $d/r < 2\bar{\alpha} \leqq 1.2\, d/r$.

This resolution function cannot be approximated by a Gaussian function with the same width at half maximum. The approach by a Gaussian function has more physical meaning than an approach by a triangle, since small effects[1]) that appear in practice tend to decrease the half width and to add low intensity tails to the resolution function; it has thus been approximated by a Gaussian function having the same maximum and the same area as $I(\alpha')$, that is, $2D/L$. Such a Gaussian function will have a full width at half maximum given by

$$\Gamma_{\frac{1}{2}} = (2D/L)(2/I_{\max})(\pi^{-1}\ln 2)^{\frac{1}{2}}. \qquad (13)$$

This result can be expressed as $\Gamma_{\frac{1}{2}} = c(d/r)$, where c varies between 1 and $\frac{8}{3}(\pi^{-1}\ln 2)^{\frac{1}{2}} \cong 1.25$, in a time scale

$$\delta t_\omega = \Gamma_{\frac{1}{2}}/\omega = c(d/r)/\omega. \qquad (14)$$

In the present experimental arrangement the collimation is determined by the very small detecting area, and we are in the above case (b). The resolution function $I(\alpha', v_0)$ has been calculated for a 1.5 m flight path and is shown in fig. 5b. The result is a curve having a maximum in 0.3512 and full width at half maximum $2\bar{\alpha} = 0.044$. This curve has been approximated to a Gaussian with $c = 1.04$, also shown in the figure.

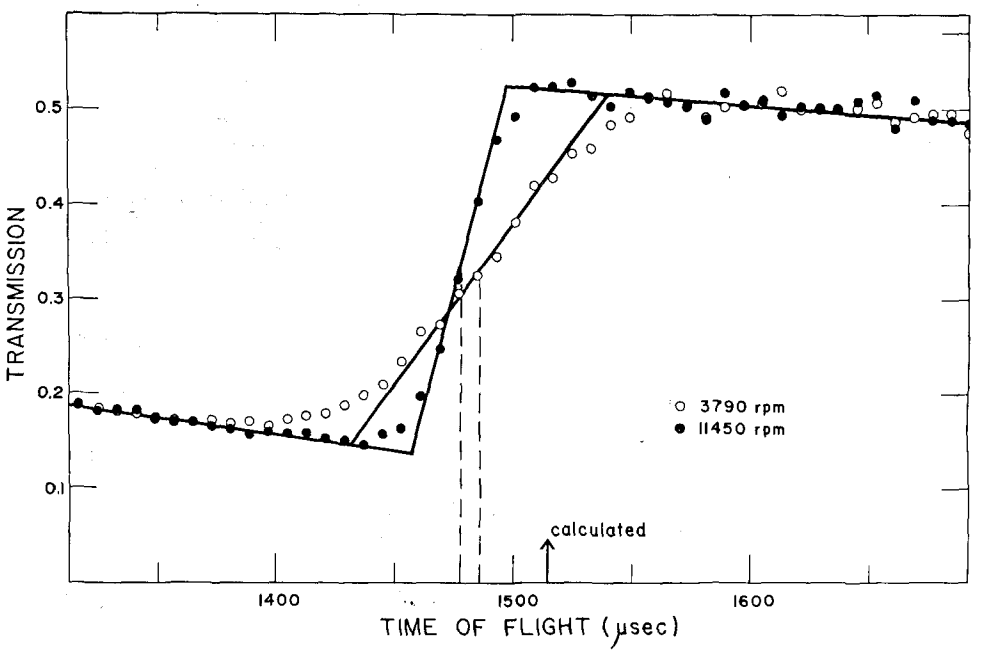

Fig. 6. Measured transmission of the Fe(110) Bragg cut-off for two different chopper speeds. These results have been used for adjusting the pick-up position and appear in one of the calibration curves of fig. 8.

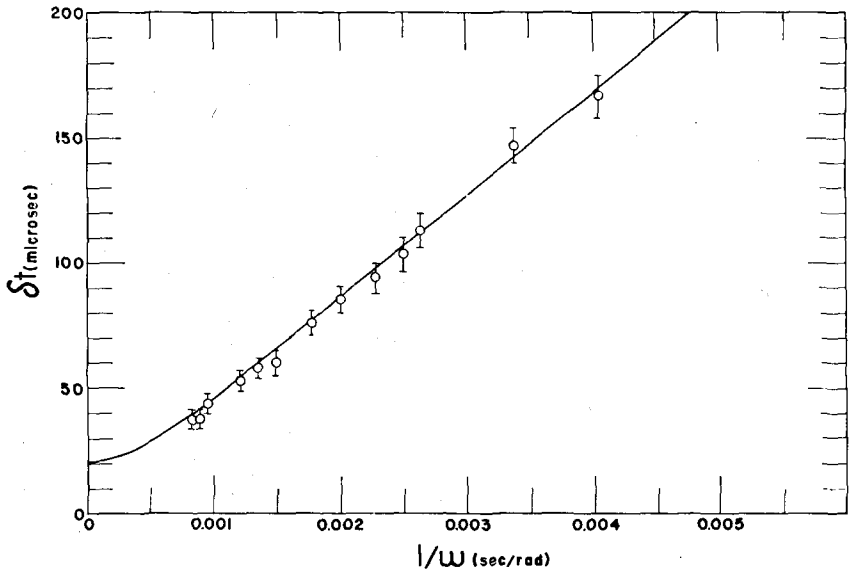

Fig. 7. Spectrometer resolution as a function of $1/\omega$: calculated curve and experimental points for 4.046 Å neutrons.

3.3. Calibration and experimental determination of the resolution

In order to obtain a zero time calibration independent of the chopper speed, and simultaneously to determine experimentally the spectrometer resolution as a function of the chopper speed, the transmission of polycrystalline iron has been measured in the region of the (110) Bragg cut-off, corresponding to 4.046 Å neutrons, for many rotation velocities. In fig. 6 transmission measurements for two chopper speeds with a 1.5 m flight path are shown as a function of time-of-flight.

The experimentally determined resolution widths as

well as the calculated curve are shown in fig. 7, as functions of $1/\omega$. The agreement is fairly good, thus indicating that the approach by Gaussian functions is valid.

For calibrating the spectrometer, the transmission curve was fitted to straight lines and eq. (9) shows that the abcissa corresponding to the half-height of the observed break is shifted from the true cut-off position by only 0.2% for the worst considered resolution. To perform a zero time calibration independent of the chopper speed, the experimentally obtained time-of-flight of the 4.046 Å neutrons was plotted against $1/\omega$. The coefficient of the straight line thus obtained is the angular shift $\Delta\phi$, and this line should pass through the calculated value for $1/\omega = 0$. Successive adjustments of the pick-up position, until the condition $\Delta\phi = 0$ was reached, are shown in fig. 8. A calibration independent of the chopper speed within 4 μsec was obtained.

A fixed displacement Δt_2 between the measured and calculated time-of-flight was observed, that seems independent of the chopper speed but varies with the distance between the pick-up coil and the disk where the magnet is located. In fig. 8, results are presented for two distances, 0.5 and 3.0 mm; for the pick-up in the closest position the shift is 38 ± 2 μsec. This effect is probably due to a non-uniform magnetic field.

After the final adjustment of the pick-up position, measurements at different wavelengths have been carried out by analysing other Fe breaks and the graphite (0002) Bragg cut-off. It was observed that the cali-

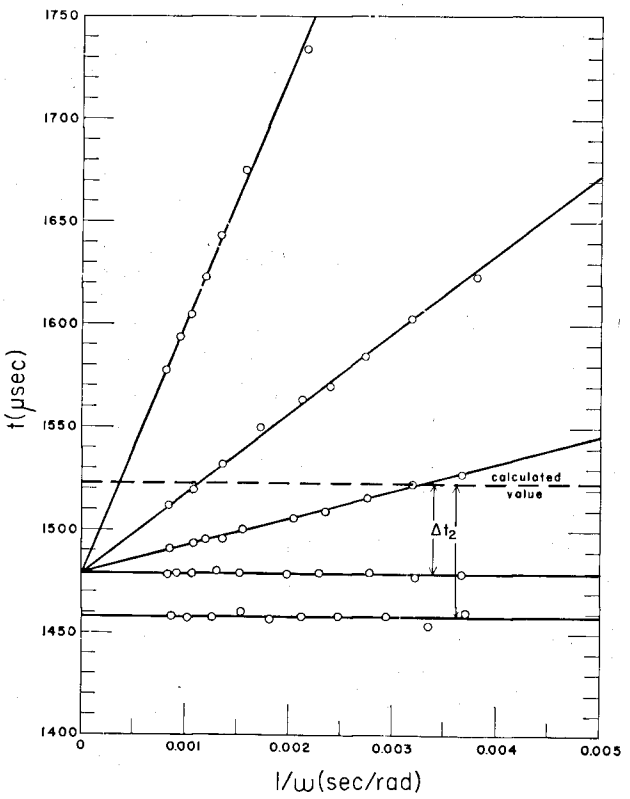

Fig. 8. Calibration curves in function of $1/\omega$. The slope of the straight line is $\Delta\phi$, and a calibration independent of chopper speed is attained for $\Delta\phi = 0$. Results are shown for two distances from the pick-up coil to the disk where the magnet is located, 0.5 and 3.0 mm.

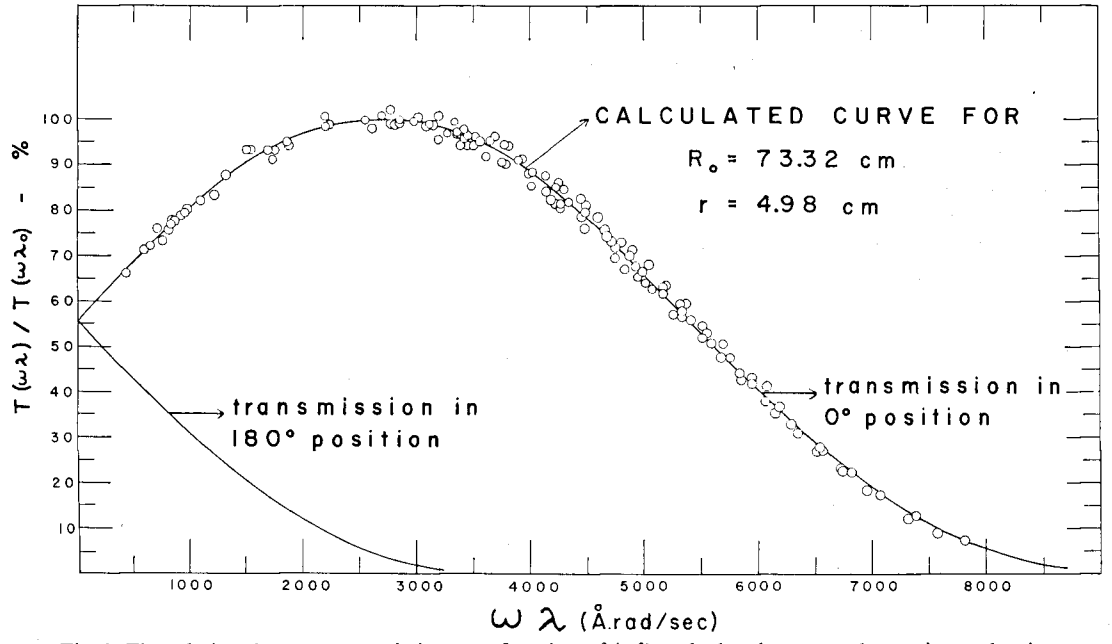

Fig. 9. The relative chopper transmission as a function of $(\omega\lambda)$; calculated curve and experimental points.

bration is independent of neutron wavelength: the break position was constant with the chopper speed and the same Δt_2 shift was observed. This experimentally determined shift has been introduced as an additive correction in the time scale.

3.4. Other important operational characteristics

The chopper transmission, obtained by integrating[1,12]) the transmission function $T(\alpha,v)$ with respect to the angle α, is a function of the product $(\omega\lambda)$. It can thus be experimentally determined by fixing one of the two variables and studying the transmitted intensity as a function of the other variable. For this, the transmitted spectrum was measured with different chopper speeds, varying from 2500 rpm to 10000 rpm. Several neutron wavelengths, from 0.8 Å to 8.2 Å have been considered; for each wavelength, the transmitted intensity as a function of $(\omega\lambda)$ gives a curve proportional to the transmission curve. These several curves after normalization give the experimental transmission function. The $(\omega\lambda)$ interval from 400 to 7800 Å·rad/sec has been covered with 29 curves, with a total of 134 experimental points. The radius of curvature R_0 has been determined from the experimental maximum observed at 2700 Å·rad/sec, thus resulting a value 73.32 cm, that presents an apparent deviation of 1.6% from the nominal design value.

The calculated[11]) curve that gave the best fit to the experimental points used an effective radius $r = 4.98$ cm for the chopper, because in our collimation the beam covers only some central slits. All the experimental curves were normalized again to this calculated one, and the final result is presented in fig. 9. The agreement between the experimental points and the theoretical curve is quite satisfactory.

The time-of-flight spectrometer here described presents a great flexibility for total neutron cross section measurements. As the chopper transmission function is relatively flat, a wide range of neutron wavelengths, from 0.5 Å up to 12 Å, can be covered by varying the chopper speed, what can be done without being necessary a new calibration. The background[11]) has a time dependent contribution that gives two maxima, corresponding to the 0° and 180° open positions of the rotor; between these maxima there are flat regions, corresponding to the time independent background. It is often possible to work in the low background region, since the neutron flight path can be easily changed; furthermore, the epi-thermal background can be reduced by using convenient filters.

The authors wish to thank Professor M. D. de Souza Santos for his continued interest and support, Dr. R. L. Zimmerman for valuable discussions, and Professor K. E. Larsson, who kindly made available the design of the slow-chopper. We also are indebted to Mr. José Ferreira for his technical assistance.

References

1) K. E. Larsson, U. Dahlborg, S. Holmryd, K. Otnes and R. Stedman, Ark. Fys. **16** (1959) 199.
2) D. J. Hughes, *Pile neutron research* (Addison-Wesley, 1953) ch. 9.
3) P. A. Egelstaff, J. Nucl. Energy **1** (1954) 57.
4) H. Ceulemans, A. Deruytter, M. Nève de Mevergnies and H. Pollak, *Pile neutron research in physics* (Conf. Proc., IAEA, Vienna, 1962) 195.
5) A. Deruytter, H. Ceulemans, M. Nève de Mevergnies and H. Moret, *Neutron time-of-flight methods* (Symp. Proc., Euratom, Brussels, 1961) 275.
6) T. Niewiadomski, A. Szkatula and J. Sciensinski, Nukleonika **7** (1962) 231.
7) K.-E. Larsson and K. Otnes, Ark. Fys. **15** (1959) 49 (appendix p. 58).
8) R. L. Zimmerman, L. Q. Amaral, R. Fulfaro, M. C. Mattos, M. Abreu and R. Stasiulevicius, Nuclear Physics A**95** (1967) 683.
9) J. M. Cassels, Progr. Nucl. Phys. **1** (1950) 185.
10) E. Fermi, J. Marshall and L. Marshall, Phys. Rev. **72** (1947) 193.
11) S. B. Herdade, L. Q. Amaral, C. Rodriguez and L. A. Vinhas, IEA Report no. 136 (1967).
12) M. Marseguerra and G. Pauli, Nucl. Instr. and Meth. **4** (1959) 140.

RESUMO

Discute-se o método de calibrar e determinar a resolução de espectrômetros para nêutrons lentos através de medidas dos degraus de Bragg. Estuda-se analìticamente a convolução de uma função de resolução gaussiana com uma função linear que apresenta um degrau descontínuo. É determinada a razão entre a "largura de degrau" resultante e a largura de resolução; em casos práticos seu valor é 1,0645. É dada uma relação entre a abcissa média, correspondente à meia altura da curva resultante, e a verdadeira posição do degrau; elas coincidem para degraus simétricos.

O efeito de uma resolução gaussiana na transmissão, no inverso da transmissão e na secção de choque total é calculado teòricamente para o degrau de Bragg (110) do ferro, para várias larguras de resolução e várias espessuras da amostra. Conclue-se que a análise da curva de transmissão medida fornece o resultado mais direto e preciso.

São apresentadas as características de um espectrômetro de tempo de vôo com um obturador de nêutrons lentos de placas curvas, construído no IEA. A resolução em tempo para as atuais condições de geometria, com uma área detetora muito pequena, é de 1% para uma distância de vôo de 3 metros e para nêutrons de 4,046 Å.

Quando há interêsse em cobrir um grande intervalo de energia, é desejável a obtenção de uma calibração independente da velocidade de rotação do obturador; isto foi conseguido dentro da precisão de 4 μseg. O espectrômetro pode ser usado para medidas de secção de choque total no intervalo de 0,5 Å até 12 Å.

RESUMÉ

On discute la méthode de calibration et détermination de la résolution des spectromètres pour neutrons lents par des mesures de "Bragg breaks". On étudie analytiquement la convolution d'une fonction de résolution gaussienne avec une fonction linéaire qui présente une descontinuité. On détermine la raison entre la largeur résultante et la largeur de résolution; dans les cas pratiques sa valeur est 1,0645. On donne une rélation entre l'abscisse moyenne, correspondante à la mi-hauteur de la courbe résultante, et la vraie position du "Bragg break"; elles ne coincident que pour des courbes symetriques.

L'effet d'une résolution gaussienne sur la transmission, sur l'inverse de la transmission et sur la section efficace totale a été calculé théoriquement pour le "Bragg cut-off" (110) du fer, avec de différentes largeurs de résolution et de différentes épaisseurs de l'échantillon. On conclut que l'analyse de la courbe de transmission mésurée donne le résultat plus direct et précis.

On présente les charactéristiques d'un spectromètre à temps de vol avec un obturateur à plaques courbes pour neutrons lents, construit à l'IEA. La résolution en temps dans les présentes conditions de géométrie, avec une très petite surface détectrice, est de 1% pour une distance de vol de 3 mètres et des neutrons de 4,046 Å. Quand il y a de l'intérêt en couvrir un grand intervalle d'énergie, c'est désirable l'obtention d'une calibration indépendante de la vitesse de rotation de l'obturateur de neutrons, ce qui a été obtenu avec la precision de 4 μsec. Le spectromètre peut être employé pour mesures de section efficace totale dans l'intervalle de 0,5 Å jusqu'à 12 Å.